Synthesis of Calcium Hexaboride Powder via Boro/ Carbothermal Reduction with a Gel Precursor

D. Yilmaz Çakta[*1], N. Koç[1], S. Turan[2]

[1]Department of Metallurgy and Materials Engineering, Eskisehir Osmangazi University, Eskisehir, Turkey.
[2]Department of Materials Science and Engineering, Anadolu University, Eskisehir, Turkey.

Abstract

In this study, the synthesis of calcium hexaboride powder via boro/carbothermal reduction (BCTR) using a single-step-processed gel product prepared from commercial boric acid, readily available and low-cost D(-)-Mannitol and calcium carbonate was investigated. The gel product was characterized by means of Fourier Transform Infrared Spectroscopy (FTIR) and Simultaneous Thermal Analysis (STA). The effect of the boro/carbothermal reduction temperature and dwell time on the phase formation were examined with x-ray diffractometry and scanning electron microscopy. CaB_6 synthesis was performed with the gel product without additional heat treatment in air to obtain the appropriate C amount in the gel precursor. $Ca_3B_2O_6$, B_4C and $Ca_2B_6O_{11}$ were formed as a transitional phase to create CaB_6 particles. To understand the formation and consuming mechanism of the transitional phases, thermodynamic calculations were performed based on reactions that probably occurred in the system. The optimum synthesis conditions for the formation of calcium hexaboride were determined as 1400 °C for 12 h in an argon flow.

Keywords: Hexaboride, boro/carbothermal reduction, gel precursor, boric acid, mannitol

I. Introduction

In recent years, the unique properties of calcium hexaboride (CaB_6), such as its high melting point, high chemical stability, high hardness and the ability of its composites to absorb neutron radiation, have attracted the attention of the researchers and related industry [1-2]. CaB_6 is a good candidate for cathode materials [3], filler material for bipolar plates in proton exchange membrane (PEM) fuel cells [4] and for other similar electronic materials owing to its low electronic work function and diverse magnetic orders [5]. It is also commonly used as an antioxidant in refractory magnesia-carbon bricks [6] and as a deoxidant in pure iron, steel and mostly in copper production owing to its minimal effect on electrical conductivity [7].

The common reported production methods for CaB_6 are: (i) the direct reaction of pure elements at high temperature and pressure [8], (ii) carbothermic-metallothermic reduction of oxides or borates [9-10], (iii) boro/carbothermic reduction [5], (iv) electrochemical synthesis [11], (v) mechanochemical synthesis [12] and (vi) reaction of compounds in an autoclave [13], etc. Since the properties of the end-product depend on the properties of the raw materials and the production method, it is important to select an appropriate method to synthesize CaB_6 [14]. Boron carbide (B_4C) is used as a starting material for CaB_6 synthesis on account of the high mass yield of CaB_6 [15]. The reaction of the metal oxide and B_4C with carbon (C) at high temperature is called boro/carbothermic reduction

(B_4C-method), in which B_4C provides both boron (B) as a reactant and C for the reduction of the oxide [9]. The reaction for the boro/carbothermal reduction (BCTR) of calcium carbonate is given below.

$$2CaCO_3 + 3B_4C + C \rightarrow 2CaB_{6(s)} + 6CO_{(g)} \qquad (1)$$

To synthesize fine CaB_6 powder, it is necessary to use fine B_4C powder. Commercially, B_4C is synthesized via carbothermal reduction (Eq. 2.) at a high synthesis temperature and the resulting B_4C ingots are crushed to produce powders. Owing to the high hardness of B_4C powder, it is difficult to obtain and use fine B_4C powders as a raw material [16]. In addition, the use of commercial B_4C as a raw material prevents the production of fine CaB_6 powder owing to aggregate formation during BCTR [15].

$$2B_2O_{3(l,g)} + 7C_{(s)} \rightarrow B_4C_{(s)} + 6CO_{(g)} \qquad (2)$$
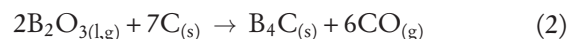
The aim of this study is to synthesize CaB_6 powder via BCTR of *in-situ*-formed transitional phases and calcium oxide (CaO) based on transient formation of B_4C and $Ca_xB_yO_z$ (calcium borates) in a gel product. To achieve *in-situ*-formed transitional phases, the BCTR technique was studied using a single-step-processed gel product that includes H_3BO_3 as a B source, D(-)-Mannitol as a C source and calcium carbonate ($CaCO_3$) as a calcium source. To synthesize boride in a one-step process with minimal secondary phases, it is important to minimize B loss by forming B-O-C bonds in the gel product. Creating B-O-C bonds in the gel product accelerates the dispersion of compounds and the synthesis temperature decreases owing to the superior activity of the enlarged surface area of the

* Corresponding author: dcakta@ogu.edu.tr

species [17]. A few studies are available on the synthesis of CaB_6 via transient B_4C formation. Coke as a C source and colemanite ($2CaO·3B_2O_3·5H_2O$) as both a Ca and B source were used as raw materials, and with this method, CaB_6 formation was observed at above 1700 °C [9]. Another reported study, which was performed at low temperature (1400 °C) based on transient B_4C formation, was aimed at synthesizing CaB_6 using a condensed product obtained from PVA-H_3BO_3. With this method, it is reported that to obtain raw materials for CaB_6 synthesis, heat treatment in air is performed for a mixture of H_3BO_3-PVA to obtain an appropriate amount of C in the condensed product, then this product was mixed with the calcium source [16]. Mannitol is a common polyol and can be classified as a sugar alcohol that is used for the titration of H_3BO_3 owing to its unique ability to form borate esters with H_3BO_3 [18]. In addition to this, Mannitol is one of the low-cost polyols for use as a C source, since sugar alcohols can be synthesized from starch and sucrose. Moreover, Turkey is one of the richest countries with regard to boron reserves and its soil contains rich calcium carbonate deposits. For these reasons, H_3BO_3 and $CaCO_3$ are readily available at relatively low cost. Starting from this point of view, D(-)-Mannitol is a good candidate to obtain transient B_4C. In this study, CaB_6 powder was synthesized via BCTR with a gel precursor. To eliminate an extra mixing step for the gel product and calcium source, $CaCO_3$, $C_6H_{14}O_6$ and H_3BO_3 were all used in a single-step process to synthesize gel and C/B_2O_3 was set directly to an approproiate ratio without heat treatment in air.

For CaB_6, there are a few sintering studies in the literature and these studies were generally performed with commercially available CaB_6 powders. It is known that submicron- to micron-scale boride powders are generally favored compared to coarser powders for use in engineering applications. Available technical grade CaB_6 powders (Table 1) have a purity between > 95 % to > 99 % and a particle size between 44 – 840 µm. In addition to this, industrial grade CaB_6 powders also can be found economically with a 20 – 50 µm particle size.

Table 1: Available CaB_6 powders.

Source	Grade	Purity	Particle Size	Price (2016)
Sigma-Aldrich™	Technical	99.5%	74 µm	80.2€/10 g
Alfa Aesar™	Technical	> 95 %	840 µm	509€/1 kg
Alfa Aesar™	Technical	99.5%	44 µm	461€/100 g
Alfa Aesar™	Technical	> 99 %	840 µm	593€/500 g
China-Mass Production	Industrial	Fe, Ti, Mg, Cu, Mn, Na, Co, Zn, Ni, Pb, K, N, C, S, O	20 µm	18 – 45€/1 kg

In this study, CaB_6 powders synthesized at 1400 °C for 12 h have a µm-size (smaller than 5 µm). In addition to this,

the raw materials used in our study are readily available raw materials. As Turkey has 74 % of the world's boron resources, they can be found locally at low price in Turkey. To summarize, owing to the powder's particle size and raw materials that used in this study, it offers many advantages.

II. Experimental

(1) Synthesis of calcium hexaboride powder

The raw materials used in this study were $CaCO_3$ (Merck, 99 %), H_3BO_3 (ETI™ Mine, 99.5 %), D(-)-Mannitol ($C_6H_{14}O_6$, Merck™, 99 %) and all of them were used as received. The precursor was prepared by means of the dehydration condensation of mixed H_3BO_3-deionized water (DIW) and D(-)-Mannitol-DIW solution in a certain molar ratio that includes excess B_2O_3 (15 %) according to the necessary C/B_2O_3 ratio for carbothermic reduction (Eq. 2) to offset the probable B_2O_3 loss. Firstly, 1 mole of D(-)-Mannitol was dissolved in 25 ml of DIW. Secondly, 4 moles of H_3BO_3 were dissolved in 1 liter of DIW (Table 2). All the solutions were stirred at 200 rpm and heated at 65 °C. After dissolution, the D(-)-Mannitol-DIW solution was added dropwise at a rate of 2 ml/min into the H_3BO_3-DIW solution. Then, 2 mole $CaCO_3$ was added to the stirred solution for every 3 mole of H_3BO_3 to obtain the appropriate ratio for boride production (Ca-CO_3:B_2O_3 = 1:3). The mixed semi-transparent solution was kept at 65 °C for 4 h and then heated until all water was evaporated at 80 °C. The resulting semi-transparent product was dried in an oven for 24 h at 100 °C.

Table 2: Chemical composition of the gel product.

H_3BO_3 (mole)	D(-)-Mannitol (mole)	$CaCO_3$ (mole)	C/B_2O_3	$CaCO_3/B_2O_3$
4	1	0.66	3	0,33

Thermal decomposition was performed at 400 °C for 2 h in an argon atmosphere. Decomposed gel product was ground with an agate mortar and pestle and pressed into pellets on a hydraulic press at 40 MPa. The pellets were placed in a graphite crucible and heated at 1300 – 1500 °C for 6 – 12 h under an argon flow at a heating rate of 10 K/min. The powders were purified using 1 M hydrochloric acid solution for 30 min to remove unreacted compounds. Then the powders were filtrated with a filter system and washed five times with hot water. At every washing step, the pH of the solution was measured and the powders were washed until the pH value was neutral.

(2) Characterization

Phase analysis of the resulting products was conducted with x-ray diffractometry (XRD-Rigaku, MiniFlex600, Rigaku Co., Ltd., Tokyo, Japan) operated at 40 kV and 15 mA with monochromated CuKα radiation. Raw materials and synthesized powders were pressed into pellets by mixing of KBr powders to investigate functional groups using Fourier Transform Infrared Spectroscopy (Bruker-Tensor 27 FTIR) in transmission mode.

Thermal analysis of the gel product was performed to obtain the decomposition temperature of the gel product with simultaneous thermal analyser (STA)-thermogravimetric analysis (TG)/differential thermal analysis (DTA) (Netzsch 449F3) and heating scans were performed up to 700 °C at a rate of 10 K/min in an argon atmosphere.

Morphology and microanalysis of the resulting powder were conducted via using scanning electron microscopy and energy dispersive spectrometer (SEM-Zeiss Supra 50 VP/EDS-Oxford INCA) operated at 15 kV. The EDS was calibrated on boron nitride grains. Samples were coated with Au-Pd before SEM imaging. Thermodynamic calculations were performed using the FactSage-Reaction Module, under presumption of non-isothermal and standard state and with using Pure Substance (FACT-SGPS), Oxide (FACT-OXID) and Elements (FACT-ELEM) databases.

III. Results and Discussion

(1) Properties of the gel product

To characterize the bonding states in the gel product, the FTIR spectrum was obtained (Fig. 1). The broad absorption peaks between 3500 and 3200 cm^{-1} were related to the stretching band of O-H groups in ester. The absorption peaks between 3000 and 2800, 1620 and 1080 cm^{-1} were attributed to C-H, C-C and C-O bands, respectively [19]. There is no absorption peak at 1195 cm^{-1}, which is related to the deformation band of B-O-H [17]. Therefore, it can be said that all boric acid in the gel product has reacted with D(-)-Mannitol and no boric acid is left in the precursor. Two absorption peaks at 1130 and 965 cm^{-1} indicated that B-O-C bonds were formed successfully [17,20]. In addition to these, peaks between 1480 and 1400 and between 850 and 650 were related to B-O bonds [17,21,22], and peaks at 875 and 1465 cm^{-1} were related to CaCO$_3$. On the basis of all this information, the FTIR spectra confirmed that gel product has been successfully formed by H$_3$BO$_3$,C$_6$H$_{14}$O$_6$ and CaCO$_3$.

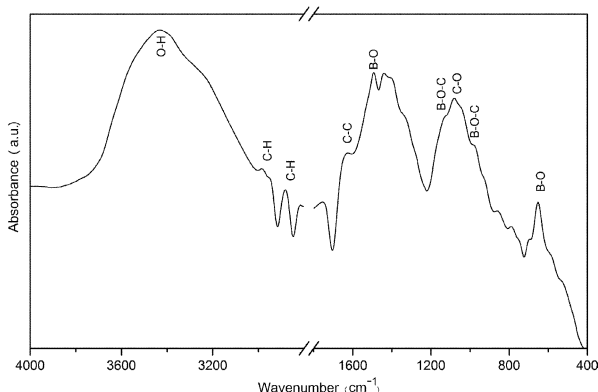**Fig. 1:** FTIR spectra of the gel product obtained from H$_3$BO$_3$-C$_6$H$_{14}$O$_6$-CaCO$_3$.

To investigate the thermal characteristics of the gel product, TG/DTA analysis were conducted simultaneously (Fig. 2). The heating rate was chosen as 10 °C/min up to 700 °C in an argon flow. The significant decomposition peak was observed approximately at 400 °C. Therefore, 400 °C was selected as an appropriate temperature for the thermal decomposition of gel product. With increasing

temperature, weight loss took place between 250 – 550 °C. There are no endothermic peaks or weight loss below 170 °C, which is the melting point of boric acid. It was also seen that there is no evidence for melting or decomposition of a boric acid in a gel product, so this means that there is no unreacted boric acid in the gel product and all boric acid in the system has been used to form borate ester with D(-)-Mannitol. There is also no endothermic peak between 450 – 550 °C, which indicates the melting point of B$_2$O$_3$. These results reveal that B-O-C bonds were formed homogeneously in the gel product.
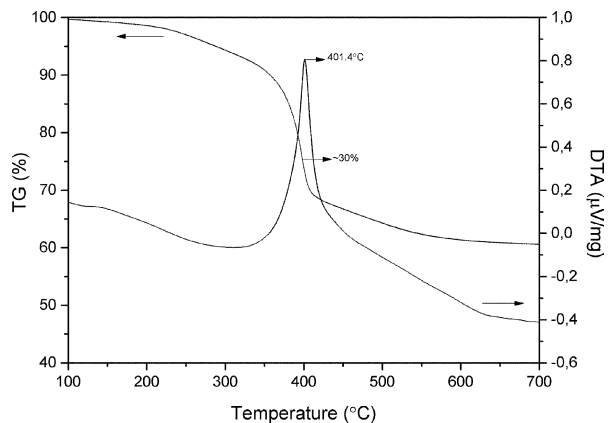

Fig. 2: TG/DTA curves of the gel product obtained from H$_3$BO$_3$-C$_6$H$_{14}$O$_6$-CaCO$_3$.

(2) Properties of the resulting powder

The formation temperature of the CaB$_6$ powder is probably related to the formation of the transitional phases (Table 3). Therefore, it is important to determine the formation temperature of the transitional phases. The main transitional phases in CaB$_6$ synthesis are Ca$_x$B$_y$O$_z$ and B$_4$C. Fig. 3 and Fig. 4 show the standard Gibbs free energy change ($\Delta G°$)-temperature relation of the formation reaction of the B$_4$C and Ca$_x$B$_y$O$_z$, respectively.
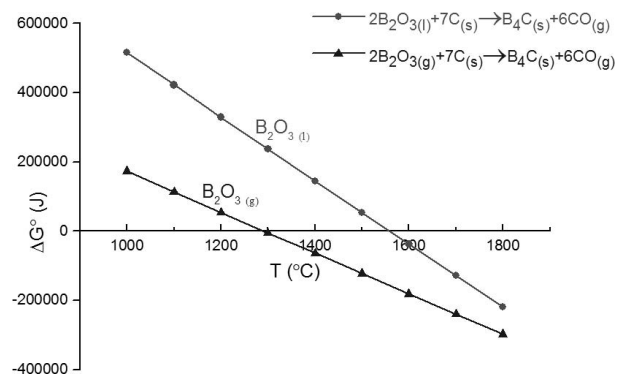

Fig. 3: Standard Gibbs free energy change ($\Delta G°$)-temperature relation of the reaction given in Eq. 2.

According to the thermodynamic data, B$_4$C formation can occur by carbothermic reduction over both liquid phase (B$_2$O$_{3(l)}$) approximately at 1550 °C and gas phase (B$_2$O$_{3(g)}$) which is in an equilibrilium with its liquid phase approx. at 1290 °C (Fig. 3). The Ca$_x$B$_y$O$_z$ formation reaction has a large negative Gibbs free energy, therefore it is obvious that the formation of calcium borates can be spontaneous and the formation of calcium-rich borates easier than that of boron-rich borates.

Table 3: Possible formation and BCTR mechanism in our work.

Scenario	Reaction
	$C_{(s)}+B_2O_{3(l,g)} \rightarrow B_4C_{(s)}+CO_{(g)}$
	$C_{(s)}+B_2O_{3(g)} \rightarrow B_4C_{(s)}+CO_{(g)}$
	$2CaO_{(s)}+3B_2O_{3(l,g)} \rightarrow Ca_2B_6O_{11(s)}$
Formation of transitional phases	$3CaO_{(s)}+B_2O_{3(l,g)} \rightarrow Ca_3B_2O_{6(s)}$
	$Ca_2B_6O_{11(s)}+CaO_{(s)} \rightarrow Ca_3B_2O_{6(s)}+B_2O_{3(l,g)}$
BCTR of transitional phases	$Ca_3B_2O_{6(s)}+4B_4C_{(s)}+2C_{(s)} \rightarrow 3CaB_{6(s)}+6CO_{(g)}$
	$Ca_2B_6O_{11(s)}+2B_4C_{(s)}+6C_{(s)} \rightarrow 2CaB_{6(s)}+B_2O_{3(g)}+8CO_{(g)}$
	$2CaO_{(s)}+3B_4C_{(s)} \rightarrow 2CaB_{6(s)}+C_{(s)}+2CO_{(g)}$
	$2CaCO_{3(s)}+3B_4C_{(s)}+C_{(s)} \rightarrow 2CaB_{6(s)}+6CO_{(g)}$
	$CaO_{(s)}+3B_2O_{3(l,g)}+10C_{(s)} \rightarrow CaB_{6(s)}+10CO_{(g)}$

Table 4: EDS microanalysis results of the powders obtained by BCTR.

	1300 °C-6h (AP)				1400 °C-6h (BP)				1400 °C-12h (AP)	
	Spectrum 1		Spectrum 2[*]		Spectrum 1		Spectrum 2		Spectrum 1	
Element	Weight (%)	Atomic (%)	Weight (%)	Atomic (%)	Weight (%)	Atomic (%)	Weight (%)	Atomic (%)	Weight (%)	Atomic (%)
C	6.06	7.12	100	100	38.54	32.26	33.98	10.89	-	-
B	62.74	81.89	-	-	19.13	25.51	43.22	50.71	73.56	91.16
Ca	31.19	10.98	-	-	18.32	10.59	9.83	3.11	26.44	8.84
O	6.06	7.12	-	-	24.01	31.64	12.97	35.29	-	-
Total	100									

[*] EDX data was taken on the large carbon particle.
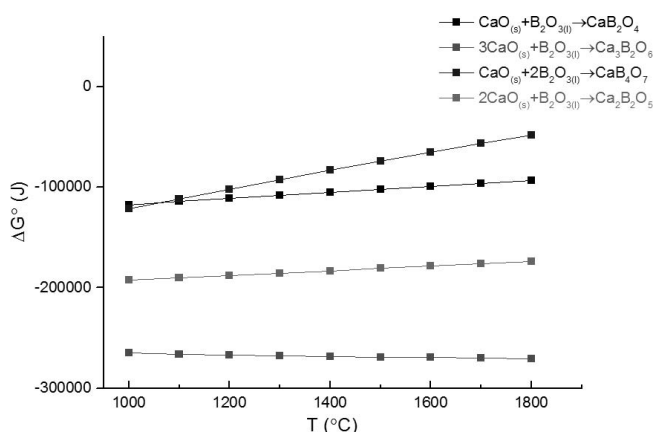
Fig. 4: Standard Gibbs free energy change ($\Delta G°$)-temperature relation of the formation reactions of $Ca_xB_yO_z$.

With reference to thermodynamic data, CaB_6 powder synthesis reactions via BCTR were performed between 1300 °C and 1500 °C. XRD patterns of powders synthesized by BCTR for 6 h at 1300, 1400 and 1500 °C are given in Fig. 5. This result indicated that CaB_6 was successfully synthesized as a single phase when BCTR was performed at 1500 °C for 6 h. However, the XRD pattern of the product obtained at 1400 °C for 6 h showed that the single-phase formation of CaB_6 was not achieved in these conditions on account of the observation of additional phases like B_4C. In addition to this, as the BCTR temperature was kept at 1300 °C, C was detected along with some B_4C (Table 4). From this, it can be seen that a dwell time longer than 6 h may be necessary at 1300 and 1400 °C to synthesize single-phase CaB_6. As a result, CaB_6 formation was firstly observed at 1300 °C and this observation was compatible with the thermodynamic data.

The effect of longer dwell times was also investigated at 1300 °C for 10 and 14 h (Fig. 6). The XRD results revealed that more than 14 h were required to synthesize single-phase CaB_6 at 1300 °C since B_4C peaks still have a high intensity in the XRD patterns of powders synthesized at 1300 °C for 14 h.

In order to understand the effect of longer dwell times, boro/carbothermal reduction was conducted at 1400 °C for 8, 10 and 12 h (Fig. 7). For the powders synthesized by means of boro/carbothermal reduction at 1400 °C for 8 and 10 h, there is still some B_4C in the powder. However, for powders synthesized at 1400 °C for 12 h, all peaks can be identified as CaB_6. Therefore, 1400 °C as a reduction temperature and 12 h as a dwell time are sufficient to synthesize single-phase CaB_6. As a result, the precursor pre-

pared from the gel H_3BO_3-D(-)Mannitol-$CaCO_3$ product by means of thermal decomposition in an argon flow is a favourable precursor for low-temperature synthesis of CaB_6 powder. In Table 5, the weight loss values of samples after BCTR and after chemical purification can be seen. As expected, after BCTR, the weight loss values of the samples increased with increasing temperature and dwell time. By-products in the system, such as suboxides and calcium borates, have high volatility owing to the high temperature, the weight loss of samples obtained at higher temperatures and dwell time is much greater than that of the samples obtained at lower temperatures. Similarly, the amount of the unreacted compounds in the samples obtained at higher temperatures and dwell time is also much higher than in samples obtained at lower temperatures. These results also reveal that the reduction completion ratios are higher at higher temperatures and dwell times.
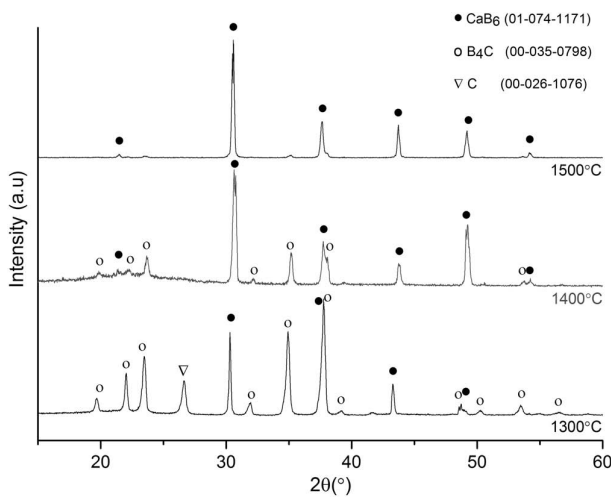

Fig. 5: XRD patterns of the products obtained by BCTR at 1300, 1400 and 1500 °C for 6 h in an argon flow.
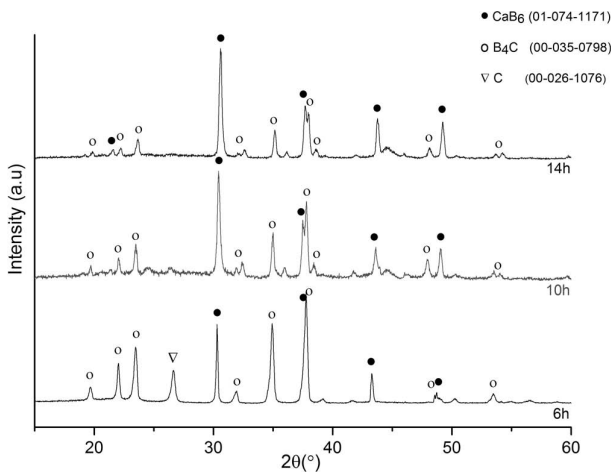

Fig. 6: XRD patterns of the powders obtained by BCTR at 1300 °C for 6 – 14 h in an argon flow.

To understand the formation and consuming mechanism of transitional phases, thermodynamic calculations were performed based on reactions that have probably occurred in the system. Fig. 8 shows the standard Gibbs free energy change ($\Delta G°$)-temperature relation of the formation reactions of CaB_6 over $Ca_xB_yO_z$, B_2O_3 and C. It is obvious that the carbothermic reduction temperature of B_2O_3 and

CaO is lower than the carbothermic reduction temperature of B_2O_3 and $Ca_xB_yO_z$. In addition to this, CaB_6 synthesis via carbothermic reduction over B_2O_3 and CaO can occur at approximately at 1300 °C theoretically, but higher temperatures are necessary if $Ca_xB_yO_z$ takes the place of CaO. In the event of boron-rich borates being present in the system, the carbothermic reduction temperature is higher compared with the carbothermic reduction of calcium-rich borates.
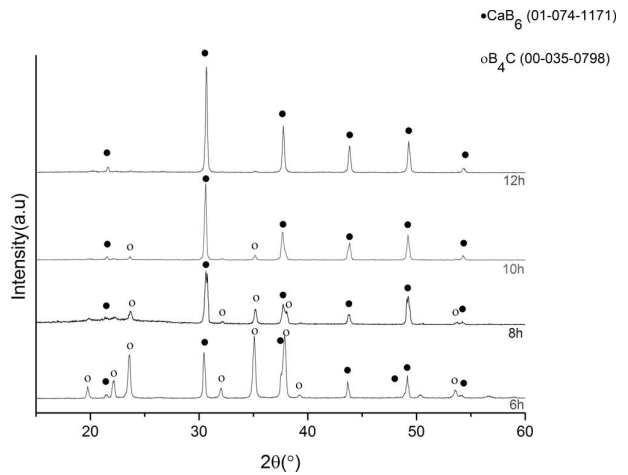

Fig. 7: XRD patterns of the powders obtained by BCTR at 1400 °C for 6 – 12 h in an argon flow.

Table 5: The weight loss of samples after BCTR and after chemical purification.

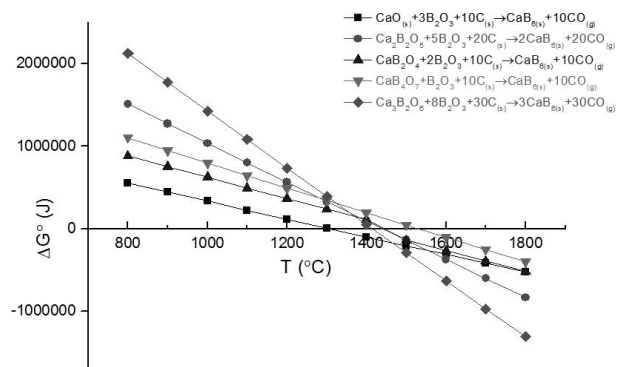| Sample	Weight Loss (%)	
	After BCTR	After chemical purification
1300 °C-6h	70.5	11.5
1300 °C-10h	72.3	8.6
1300 °C-14h	73.2	7.4
1400 °C-6h	81.8	6.2
1400 °C-8h	82.2	4.5
1400 °C-10h	84.6	3.7
1400 °C-12h	84.9	1.3
1500 °C-6h	89.7	0.8

Fig. 8: Standard Gibbs free energy change ($\Delta G°$)-temperature relation of the formation reactions of CaB_6 over $Ca_xB_yO_z$, B_2O_3 and C.

In Fig. 9, the standard Gibbs free energy change ($\Delta G°$)-temperature relation of the formation reactions of CaB_6 via BCTR can be seen. CaB_6 synthesis via BCTR over CaO can occur at approximately 1400 °C theoretically. In contrast to the carbothermic reduction of B_2O_3 and $Ca_xB_yO_z$, it can be seen that the reduction of boron-rich borates take place easily compared with the reduction of calcium-rich borates.
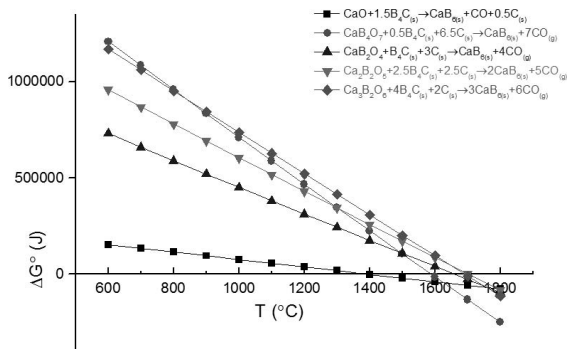
Fig. 9: Standard Gibbs free energy change ($\Delta G°$)-temperature relation of the formation reactions of CaB_6 via BCTR.
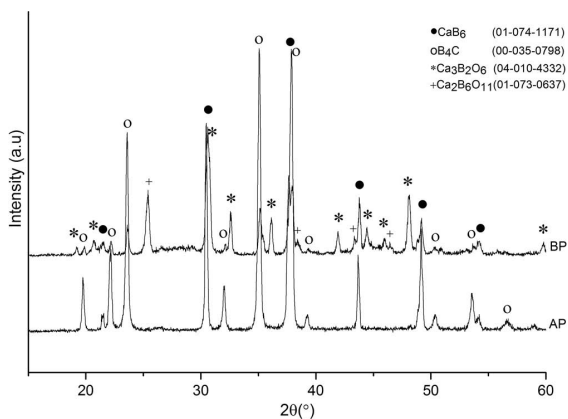
Fig. 10: XRD patterns of the powders synthesized by BCTR at 1400 °C for 6 h: (a) before purification (BP) and (b) purified with hydrochloric acid leaching (AP).

Fig. 10 shows the XRD patterns of powders before and after purification with acid leaching. It is known that $CaCO_3$ can be decomposed to calcium oxide above 800 °C. After decomposition, CaO reacts with other substances in the system to create transitional phases. It is also obvious that in the gel product, first transitional phases such as $Ca_3B_2O_6$, $Ca_2B_6O_{11}$ and B_4C were formed from calcium, B and C sources at 1300 °C, which was compatible with the thermodynamic data. In the gel precursor, $CaO:B_2O_3$ was chosen as 1:3. Therefore, CaB_6O_{10} may be expected to occur as a transitional phase, but it is known that calcium-rich borates have a higher negative Gibbs free energy, especially $Ca_3B_2O_6$, so probably Eq. 3 and Eq. 4 occur during the process.

$$CaO_{(s)} + CaB_6O_{10(s)} \rightarrow Ca_2B_6O_{11(s)} \qquad (3)$$

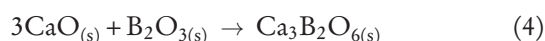$$3CaO_{(s)} + B_2O_{3(s)} \rightarrow Ca_3B_2O_{6(s)} \qquad (4)$$

Fig. 11 shows an SEM micrograph of powder obtained by means of BCTR at 1400 °C for 6 h prior to purification by means of hydrochloric acid leaching. It is obvious that the particles belonging to *in-situ*-formed tran-

sitional phases are submicron in size. It is known that fine starting materials are needed to synthesize fine boride particles. Therefore, submicron-sized *in-situ*-formed particles are also important for the BCTR process. In Table 4, EDS spectrum results taken from two different points are given. Spectrum 1 and Spectrum 2 reveal the following chemistries by wt%, respectively: 38.54 wt% C, 19.13 wt% B, 18.32 wt% Ca, 24.01 wt% O and 33.98 wt% C, 43.22 wt% B, 9.83 wt% Ca, 12.97 wt% O. The EDS spectrum results show that transitional phases were homogeneously dispersed.
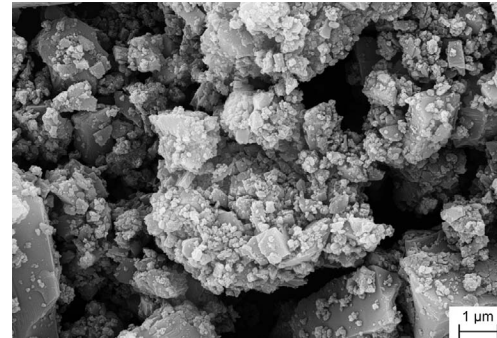
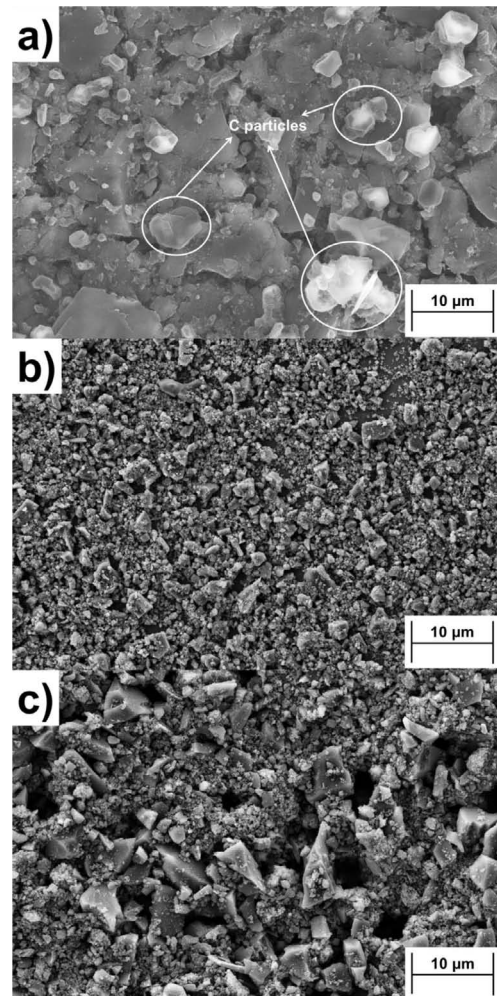**Fig. 11:** SEM micrograph of the powder obtained by BCTR at 1400 °C for 6 h (BP).

Fig. 12: SEM micrographs of the powders obtained by BCTR at a) 1300 °C, b) 1400 °C and c) 1500 °C for 6h.

Fig. 12(a)-(c) show the SEM images of CaB_6 powders synthesized for 6 h at 1300 – 1500 °C. In powders synthe-

sized at 1300 °C for 6 h, the residual C could be recognized both in Fig. 5 and arrowed in the SEM images in Fig. 12(a).

Powder sizes obtained at 1400 °C for 6 h were smaller than those obtained at 1500 °C for 6 h; but the reduction at 1400 °C for 6 h was not sufficient for the formation of single-phase CaB_6. Fig. 13 shows SEM images of powders obtained by means of boro/carbothermal reduction at 1400 °C for 12 h.

When the reduction was completed at a sufficient dwell time, the particles were coarse. Particle size of powders obtained at 1500 °C was a few micrometers; but the distribution of particle sizes was not homogeneous owing to the formation of transitional phases. It was known that the reduction temperature and dwell time influence the particle size and the formation of second phases. As a result, CaB_6 powders obtained at 1400 °C for 12 h were fine compared to powders obtained at 1500 °C for 6 h. At high magnifications, it can be seen that CaB_6 has a few hundred nanometer-size particles with a smooth surface and smaller sub-particles. EDS microanalysis of powder obtained by BCTR at 1400 °C for 12 h can be seen in Table 4. The elemental analysis was conducted as Spectrum 1. The EDS spectrum shows the following chemistries: 73.56 wt% B, 26.44 wt% Ca. These results reveal that there are only Ca and B in the system.
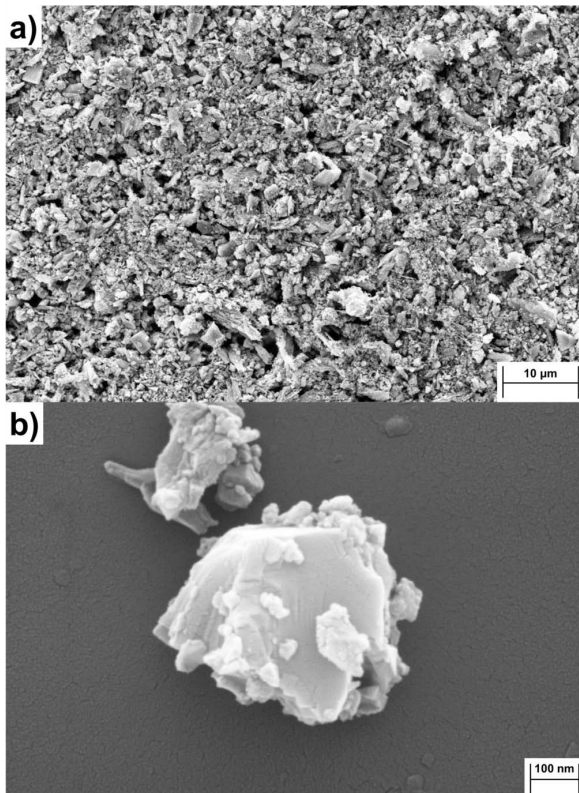
Fig. 13: SEM micrographs of powders obtained by BCTR at 1400 °C for 12 h with: a) low and b) high magnification.

IV. Conclusions

In this study, a simple method was developed to synthesize CaB_6 via BCTR from a gel precursor that was obtained from low-cost, readily available $C_6H_{14}O_6$, $CaCO_3$ and commercial H_3BO_3 from local sources. To obtain the gel precursor, the raw materials were mixed in a single step and dehydration gelation was performed. CaB_6 powder could be synthesized by means of boro/carbothermal reduction without the existence of secondary phase, and without the need for expensive raw materials such as B_4C or extra steps such as mixing of raw materials. $Ca_3B_2O_6$, B_4C and $Ca_2B_6O_{11}$ were formed as a transitional phase to create CaB_6 particles and these results were compatible with the thermodynamic data. CaB_6 was formed at 1300 °C for 6 h; but the residual C and some B_4C were also present in the powder in these conditions. Single-phase CaB_6 powder could be synthesized at 1500 °C for 6 h or at 1400 °C for 12 h by means of boro/carbothermal reduction.

References

1   Matkovich, V.I.: Boron and Refractory Borides, Springer Verlag, Berlin, 1977.

2   Tsushinsha, N.: Handbook on High-Melting Point Composites, Ehime, Japan, 1977.

3   Wang, L., Xu, L., Ju, Z., Qian, Y.:A versatile route for the convenient synthesis of rare-earth and alkaline-earth hexaborides at mild temperatures, *CrystEngComm.*, **12**, 3923 – 3928, (2010).

4   Siddiqui, N., Koc, R., Mawdsley, J., Carter, D.: Synthesis of submicron/nano sized CaB_6 from carbon coated precursors, in Nanostructured Materials and Nanotechnology V, Ceramic Engineering and Science Proceedings, Vol. 32 (eds S. Mathur, S.S. Ray, S. Widjaja and D. Singh), John Wiley & Sons, Inc., 137, 2011.

5   Zheng, S., Min, G., Zou, Z., Yu, H., Han, J.: Synthesis of calcium hexaboride powder via the reaction of calcium carbonate with boron carbide and carbon, *J. Am. Ceram. Soc.,* **84**, 2725 – 2727, (2001).

6   Hanagiri, S., Harada, T., Aso, S. *et al.*: Effects of the addition of metal and CaB_6 to magnesia carbon bricks for converters, *Taikabutsu Overseas*, **13**, 20 – 27, (1993).

7   Razavi-Zadeh, H., Mirdamadi, S.T.: Deoxidizing copper with CaB_6, *JOM*, **39**, 42 – 47, (1987).

8   Xin, S., Han, X., Liu, S., Liu, Z., Xu, B., Tian, Y., Yu, D.: CaB_6 single crystals grown under high pressure and high temperature, *J. Cryst. Growth*, **313**, 47 – 50, (2010).

9   Yildiz, O., Telle, R., Schmalzried, C., Kaiser, A.: Phase transformation of transient B_4C to CaB_6 during production of CaB_6 from colemanite, *J. Eur. Ceram. Soc.*, **25**, 3375 – 3381, (2005).

10 Huang, X., Zhong, J., Dou, L., Wang, K.: Combustion synthesis of CaB_6 powder from calcium hexaborate and mg, *Int. J. Refract. Met. H.,* **28**, 143 – 149, (2010).

11 Angappan, S., Helan, M., Visuvasam, A., Berchmans, L.J., Ananth, V.: Electrolytic preparation of CaB_6 by molten salt technique, *Ionics,* **17**, 527 – 533, (2011).

12 Balcı, Ö., Ağaoğulları, D., Duman, İ., Öveçoğlu, M.L.: Synthesis of CaB_6 powders via mechanochemical reaction of Ca/B_2O_3 blends, *Powder Technol.*, **225**, 136 – 142, (2012).

13 Shi, L., Gu, Y., Chen, L., Yang, Z., Ma, J., Qian, Y.: Low temperature synthesis and characterization of cubic CaB_6 ultrafine powders, *Chem. Lett.*, **32**, 958 – 959, (2003).

14 Etourneau, J., Mercurio, J.P. and Hagenmuller, P.: *Compounds based on octahedral units: Hexaborides and tetra borides*, in:

V.I. Matkovitch (ed.), Boron and Refractory Borides, Springer Berlin Heidelberg, New York, 1977.

[15] Zhang, L., Min, G., Yu, H., Chen, H., Feng, G.: The size and morphology of fine CaB_6 powder synthesized by nanometer $CaCO_3$ as reactant, *Key Eng. Mat.*, 326 – 328, 369 – 372, (2006).

[16] Kakiage, M., Shiomi, S., Yanase, I., Kobayashi, H.: Low-temperature synthesis of calcium hexaboride powder via transient boron carbide formation, *J. Am. Ceram. Soc.*, **98**, 2724 – 2727, (2015).

[17] Kakiage, M., Tominaga, Y., Yanase, I., Kobayashi, H.: Synthesis of boron carbide powder in relation to composition and structural homogeneity of precursor using condensed boric acid-polyol product, *Powder Technol.*, **221**, 257 – 263, (2012).

[18] Steinberg, H.: Organoboron chemistry, Boron-oxygen and boron-sulfur compounds, **(1)**, John Wiley & Sons Inc., New York, 1964.

[19] Silverstein, R.M., Webster, F.X., Kiemle, D.J., Bryce, D.L.: Spectrometric Identification of Organic Compounds, John Wiley & Sons, Inc., 2005.

[20] Yanase, I., Ogawara, R., Kobayashi, H.: Synthesis of boron carbide powder from polyvinyl borate precursor, *Mater. Lett.*, **63**, 91 – 93, (2009).

[21] Najafi, A., Golestani-Fard, F., Rezaie, H.R., Ehsani, N.: Effect of APC addition on precursors properties during synthesis of B_4C nano powder by sol-gel process, *J. Alloy Compd.*, **509**, 9164 – 9170, (2011).

[22] Mondal, S., Banthia, A.K.: Low-temperature synthetic route for boron carbide, *J. Am. Ceram. Soc.*, **25**, 287 – 291, (2005).